JACS
JOURNAL OF THE AMERICAN CHEMICAL SOCIETY
Communication
pubs.acs.org/JACS

Pathway Selection in Peptide Amphiphile Assembly

Peter A. Korevaar,[†] Christina J. Newcomb,[‡] E. W. Meijer,*[,†] and Samuel I. Stupp*[,‡,§,∥,⊥]

[†]Institute for Complex Molecular Systems and Laboratory of Macromolecular and Organic Chemistry, Eindhoven University of Technology, 5600 MB Eindhoven, The Netherlands

[‡]Department of Materials Science and Engineering and [∥]Department of Chemistry, Northwestern University, Evanston, Illinois 60208, United States

[§]Institute for BioNanotechnology in Medicine and [⊥]Department of Medicine, Northwestern University, Chicago, Illinois 60611, United States

Supporting Information

ABSTRACT: The nature of supramolecular structures could be strongly affected by the pathways followed during their formation just as mechanisms and final outcomes in chemical reactions vary with the conditions selected. So far this is a largely unexplored area of supramolecular chemistry. We demonstrate here how different preparation protocols to self-assemble peptide amphiphiles in water can result in the formation of different supramolecular morphologies, either long filaments containing β-sheets or smaller aggregrates containing peptide segments in random coil conformation. We found that the assembly rate into β-sheets decreases in the presence of a destabilizing "good" solvent like hexafluoroisopropanol (HFIP) and is affected by transient conditions in solution. Also the peptide amphiphile investigated spontaneously nucleates the β-sheet-containing filaments at a critical fraction of HFIP in water below 21%. Furthermore, β-sheet assemblies have a high kinetic stability and, once formed, do not disassemble rapidly. We foresee that insights into the characteristic dynamics of a supramolecular system provide an efficient approach to select the optimum assembly pathway necessary for function.

Peptide amphiphiles (PAs) are a promising class of self-assembling supramolecular materials for biomedical applications.[1] Assembling PA molecules into long, rigid nanofibers yields scaffold materials that can support cells and, when functionalized with bioactive epitopes, can signal cells for differentiation[2] or proliferation.[3] *In vivo* studies have demonstrated the efficacy of bioactive PAs in spinal cord injury,[4] formation of blood vessels,[5] and regeneration of bone[6] and cartilage.[7] In order to program PAs for self-assembly into nanofibers in water, their molecular design typically comprises an aliphatic tail, a peptide segment suitable for β-sheet formation, and a peptide segment containing amino acids with charged side groups. The charged amino acids make the PA nanostructures water-soluble, whereas their assembly is induced by desolvation of the apolar tails, supported by dispersive interactions among these tails and β-sheet formation via hydrogen bonding among the hydrophobic oligopeptide blocks.[8] Modeling studies have shown that the subtle interplay between the latter two types of interactions is critical to the morphology of the assemblies, varying from single β-sheets to spherical or long cylindrical supramolecular aggregates.[9] A decade of experience with PA assemblies has resulted in several methodologies to obtain the PA fibers in aqueous solution.[7,10] The development of all these different preparation protocols emphasizes that the pathway selected to create these materials is critical to their morphology.

The formation of molecular aggregates in water normally begins by dissolving material molecularly in a "good" solvent. Subsequently, the assembly is induced by switching to "poor" solvent conditions that can be obtained by changing parameters like pH, temperature, and salt concentration or by the addition of water to the monomers that are dissolved in a cosolvent.[11] This implies that the assemblies are formed while going from good to poor solvent conditions and that conditions temporarily encountered by the system during this process can significantly affect the morphology of the structures as well. Therefore, noncovalent synthesis of assemblies in water can be very dependent on the exact preparation methodology that is applied, similar to organic synthesis.[12]

We demonstrate here how different preparation protocols result in different outcomes of the PA assembly process. We investigated the assembly of palmitoyl-$V_3A_3E_3$-NH_2, PA1 (Figure 1a), which is assumed to be molecularly dissolved in hexafluoroisopropanol (HFIP) and forms long cylindrical nanostructures in pure water[13] (Figure 1b). Here, HFIP is considered as a good solvent that preferentially solvates the aliphatic tail and the hydrophobic side chains of the oligopeptide. Although water is a better hydrogen-bond donor and acceptor, it facilitates desolvation of the apolar tail and thereby acts as a poor solvent.[14] To characterize a typical preparation of PA assemblies induced by a change from good to poor solvent conditions, we studied the assembly of PA1 (50 μg/mL) in mixtures of HFIP and water, using circular dichroism (CD) and UV spectroscopy.

In the CD and UV spectra, three solvent-composition regimes can be recognized (Figure 1c). In pure HFIP, a CD spectrum with a negative maximum at 200 nm is obtained, indicating a random coil conformation of the oligopeptides. In more aqueous solutions of, e.g. 10% (i.e., vol %) HFIP, β-sheet-like CD spectra are obtained, and concomitantly a clear red-shift appears in the UV spectrum (Figure S1). Intermediate water/HFIP fractions (e.g., 50% HFIP) result in red-shifted random coil type CD

Received: April 18, 2014
Published: June 9, 2014

   dx.doi.org/10.1021/ja503882s | J. Am. Chem. Soc. 2014, 136, 8540−8543

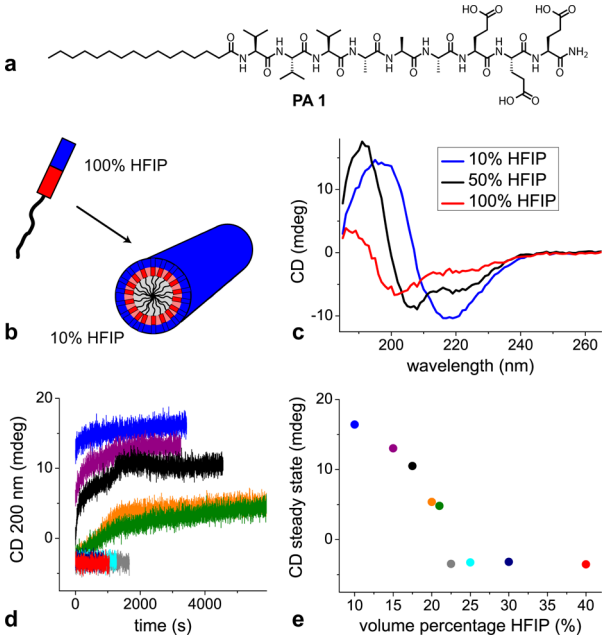

Figure 1. Dynamics and stability of PA assemblies depends on the solvent composition. (a) Molecular structure of PA1. (b) Schematic showing that PA1 is molecularly dissolved in pure HFIP and assembles under aqueous conditions via β-sheet formation into filamentous aggregates. (c) CD spectra of PA1 in 10% HFIP/90% water, 50% HFIP/50% water, and 100% HFIP. (d, e) Assembly kinetics of the β-sheets were followed in CD, revealing a decreasing rate upon increasing the HFIP content. Beyond the critical HFIP content (21 vol %), no β-sheets are formed (50 μg/mL, 20 °C, the colors of the kinetic curves in panel d correspond to the colored dots indicating the CD value in panel e).

spectra. Detailed analysis with dynamic light scattering (DLS) and small-angle X-ray scattering (SAXS) reveals that larger filament-like PA assemblies are present in solution (Figures S2 and S3) only under solvent conditions where β-sheets are obtained (<20% HFIP). Such nanofiber assemblies have anisotropic characteristics as suggested by their alignment in Couette flow (Figure S4). Furthermore, only under these conditions a hydrophobic core is formed, as evidenced by the inclusion of the solvatochromic dye nile red (Figure S5). We propose that the shifted random coil spectrum in intermediate HFIP compositions is related to either different conformational states of the PA or to the formation of small, oligomeric assemblies, since DLS does not reveal the formation of any structures (Figure S2).[15]

To further investigate the formation of β-sheets that is dependent on solvent composition, PA1 dissolved in HFIP was manually injected into water. Simultaneously, different amounts of pure HFIP were added to adjust composition. Subsequently, the formation of β-sheets in time was probed using CD and UV at 200 nm (Figures 1d and S6). All kinetic experiments with different water/HFIP ratios were performed at a total PA1 concentration of 50 μg/mL. The CD data acquired under steady-state conditions (Figure 1e) show that β-sheets (i.e., positive CD at 200 nm) only appear below 21% HFIP. At higher HFIP contents the random coils (i.e., negative CD at 200 nm) appear immediately after the injection, and both in CD and UV further changes are not observed in time. Remarkably, the kinetic curves show a minimum rate in the formation of β-sheets at the critical HFIP content of 21%.

The slowest assembly rate at the critical HFIP percentage holds an intriguing similarity to the folding and unfolding of proteins in the presence of a denaturant like urea, where minimum rates are obtained at the denaturant concentration corresponding to the thermodynamic midpoint of the denaturation curve.[16] Furthermore, kinetic studies are reported on the assembly of natural polypeptides that display a slower appearance of β-sheets in the presence of higher amounts of HFIP as well, whereas beyond a certain HFIP content only α-helices are formed.[17] Recently, we reported that also the disassembly of π-conjugated oligo(p-phenylenevinylene) assemblies has a minimum equilibrium rate at the critical good/poor solvent ratio.[18] By developing kinetic models, we unraveled that the minimum assembly or disassembly rate close to the critical solvent composition is related to the nucleation step—required to form assemblies—that becomes more hampered in the presence of a larger content of destabilizing, "good" solvent.

To illustrate the importance of the preparation protocol, we prepared a sample of the same composition in two different ways. The kinetic effects discussed above have a significant influence on the preparation of an aqueous solution of PA1 (50 μg/mL) in 20% HFIP. Even though both solutions, prepared via different methods as shown in Figure 2a, have the same HFIP and PA content, clear differences can be observed between the CD spectra of solution 1 and 2 (Figure 2b). Solution 1 yields a random coil CD spectrum, whereas the spectrum acquired on solution 2 has β-sheet character. The presence of β-sheets in solution 2 can be rationalized by the fact that for this solution first the stock solution of PA1 in HFIP is added to water. After this addition step, i.e., in the presence of 10% HFIP, PA1 forms β-sheets as evidenced by the CD spectrum of solution 2■. After the addition of the remaining amount of pure HFIP, i.e., in 20% HFIP, these β-sheets do not disassemble completely. To characterize the stability of these β-sheets in the presence of 20% HFIP in solution 2, the CD spectrum was followed in time at 200 nm. However, a transition back to random coil conformation was not observed. Conversely, we did not observe conversion

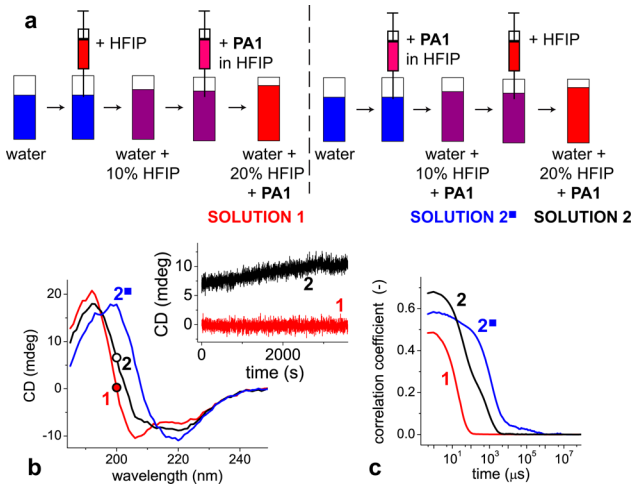

Figure 2. Assembly of PA1 is dependent on the preparation protocol. (a) Two PA1 solutions (50 μg/mL) in 20% HFIP were prepared via two methods that differ by the order in which pure HFIP and the PA/HFIP stock solution were added to water. Even though both solutions 1 and 2 contain the same PA concentration and HFIP content, clear differences can be observed in CD (b) and DLS (c). Time-dependent CD (200 nm) acquired on solutions 1 and 2, shown in the inset of panel b, demonstrates the large hysteresis involved.

dx.doi.org/10.1021/ja503882s | J. Am. Chem. Soc. 2014, 136, 8540−8543

from random coils to β-sheets for solution 1, where first pure HFIP was added to water, followed by the PA1 solution (Figure 2b). These results demonstrate that the β-sheets formed by PA1 are sensitive to hysteresis. Once formed in a solution with 10% HFIP, as evidenced by the spectrum of solution 2■, these structures do not disassemble on an observable time scale when the HFIP content is increased to 20%. The hysteresis of β-sheets in solution 2 is corroborated by DLS experiments (Figure 2c), which reveal for solution 2 correlation at much larger time scales as compared to solution 1, indicating that larger structures are present in solution 2.

To illustrate the nonlinear relation between assembly rate and solvent composition, as shown in Figure 1d, together with the hysteresis effect as shown in Figure 2, we prepared four solutions of equal PA1 concentration (93 μg/mL) and HFIP content (20%). Again, both pure HFIP as well as a stock solution of PA1 in HFIP were added to water, in four different ways as schematically depicted in Figure 3a. However, in this case the addition steps were performed right after each other, within 10–20 s, meaning that after homogenizing of the solution the next addition was performed. As shown in Figure 3b, the resulting kinetic curves for solutions 1 and 2 are similar, but solutions 3 and 4 yield different kinetic curves and even different final CD spectra (Figure 3c). These differences can be rationalized by two effects that play a key role: (1) the rate of the assembly process decreases in the presence of a destabilizing solvent like HFIP, and (2) the formed β-sheets have a high kinetic stability and, once formed, do not rapidly fall apart when more HFIP is added (i.e., hysteresis). Combining these two effects implies that if the PAs during injection from HFIP into the water phase (temporarily) experience a pure water environment, as is likely the case for solution 1, they will quickly form β-sheets. Due to the large hysteresis, these β-sheets do not directly fall apart if another 15% HFIP is added to the solution. However, if the PAs are injected in a solution that contains 15% HFIP, the driving force for making β-sheets is much smaller, and hence random coil spectra are obtained, as is the case for solution 4. Especially when the final HFIP content approximates the critical solvent composition, this hysteresis effect will have major consequences for the assembly process. Vice versa, this implies that an accurate determination of the critical solvent composition, Figure 1e, is also subject to subtle effects in the injection and mixing methodology applied.

Often it is assumed that hysteresis effects can be erased by heating the assemblies, as the fast dynamics at elevated temperatures allow entrapped monomers to re-equilibrate or disassemble. To analyze if this is the case for PA1 assemblies, we prepared PA1 solutions (50 μg/mL) at 50 °C with varying HFIP compositions of 10%, 15%, and 20%. Then, the solutions were cooled to 0 °C and subsequently heated again to 50 °C with a temperature ramp of 1 °C/min, while the assembly was analyzed with CD (Figure 4a,b). As shown in Figure 4, cooling and heating does not significantly affect the morphology of the assemblies in the solution that contains 10% HFIP: β-sheets are formed immediately at 50 °C, and these assemblies do not disappear upon cooling to 0 °C and heating back to 50 °C as evidenced by the CD spectra acquired at these temperatures. In the presence of 20% HFIP, random coil structures are obtained at 50 °C, and again the cooling and heating run does not significantly change the morphology (Figure 4c). For the PAs in 15% HFIP however, cooling the random coils that are initially obtained after the preparation of the sample at 50 °C yields around 40 °C a clear transition from random coils to β-sheets (Figure 4b). After the cooling–heating run, again with a temperature ramp of 1 °C/min, these β-sheets are still present as demonstrated by the CD spectrum acquired at 50 °C; a clear sign of hysteresis (Figure 4c). The stability of both states at 50 °C was assessed in time. For a freshly prepared solution of PA1 (50 μg/mL) at 50 °C in 15% HFIP, no changes in CD are observed (Figure 4d). However, also for a similar solution that has been subjected to a cooling–heating run, the β-sheets do not disappear at 50 °C. Formally,

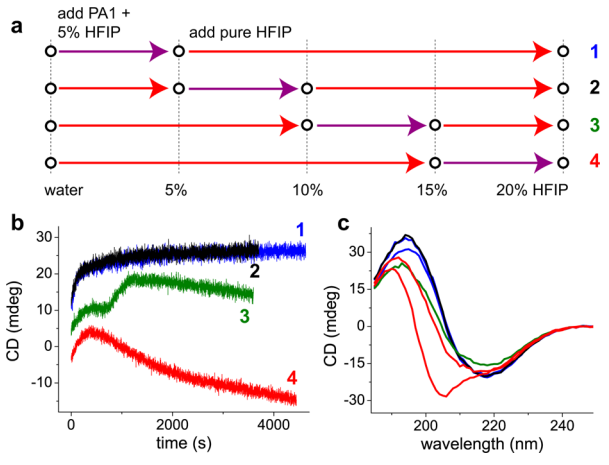

Figure 3. Four PA1 solutions (93 μg/mL) in 20% HFIP were prepared by adding 5% PA1/HFIP and aliquots of pure HFIP to water, in different order (a). Purple arrows indicate the addition of the PA1/HFIP stock solution; red arrows indicate the additions of pure HFIP to the aqueous solution. Black circles at 5%, 10%, and 15% HFIP represent intermediate stages, at which the solution is homogenized for only 10–20 s. (b) CD (200 nm) vs time after the preparation of solutions 1–4. (c) CD spectra acquired after the respective time course measurements.

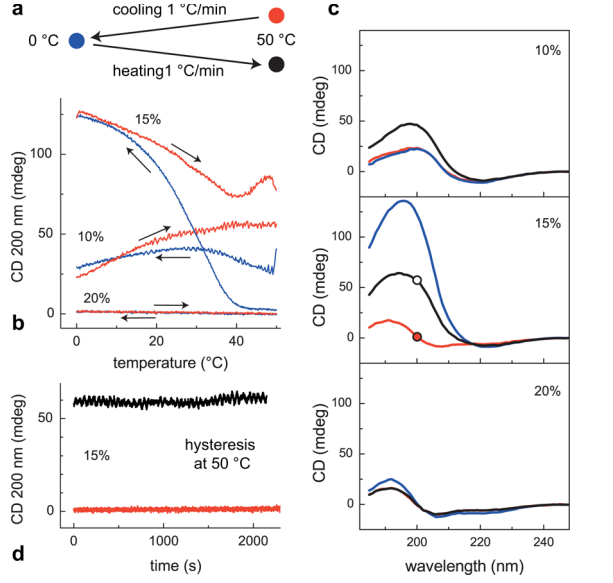

Figure 4. Temperature-dependent assembly of PA1 in different water/HFIP ratios. (a) Solutions were prepared at 50 °C (red), subsequently cooled to 0 °C (blue) and, to analyze the effect of hysteresis, subsequently heated back to 50 °C (black). (b) CD vs temperature, during cooling (blue) and heating (red) of different PA solutions (50 μg/mL) with a temperature ramp of 1 °C/min. (c) CD spectra that are subsequently acquired at 50 °C before cooling (red), at 0 °C (blue) and at 50 °C after the cooling–heating run (black) display a large hysteresis for the PA solution that contains 15% HFIP, as evidenced by time-dependent CD (d).

dx.doi.org/10.1021/ja503882s | J. Am. Chem. Soc. 2014, 136, 8540–8543

this experiment does not elucidate the equilibrium morphology under these conditions (15% HFIP, 50 °C). However, these results do emphasize that even at elevated temperatures a large hysteresis can be involved in the formation of these β-sheets: at 50 °C they cannot be formed in 15% HFIP, but once they have been formed upon cooling, they do not disassemble again at this elevated temperature.[19]

In summary, these experiments show that kinetic effects like hysteresis or the influence of solvent composition on the dynamics of the assemblies can have a strong impact on the supramolecular structures obtained. Due to these effects, conditions temporarily encountered during the preparation of the assemblies exert their influence on the morphology obtained—a phenomenon that we also encountered when analyzing these structures with electron microscopy (Figures S7 and S8). We hypothesize that the dynamic effects demonstrated here can affect the preparation of other PA systems as well, even if their assembly is controlled by other parameters like pH, salt concentration or the addition of coassembling molecular components. Hence, selecting the right pathway required for function requires an optimized preparation protocol that can be very dependent on the molecular design. For example, performing the experiments with another PA in which the final amide group at the hydrophilic end, as present in PA1, has been replaced by a carboxylic acid results in structures that are less sensitive to hysteresis (Figures S9−S11). Analyzing the dynamics of the system of interest requires a lot of experiments. Nevertheless, we foresee that understanding the effect of kinetics and hysteresis—especially on the short time scale of obvious preparation steps like injection and mixing—will enhance our ability to precisely control the self-assembly in water of amphiphiles that exhibit strong intermolecular interactions. The experiments described here demonstrate that noncovalent or supramolecular synthesis requires the same type of careful selection of preparation protocols normally associated with covalent organic and polymer synthesis. This is particularly important when the targeted function is highly dependent on supramolecular structure.

■ ASSOCIATED CONTENT

Supporting Information

Experimental details and data. This material is available free of charge via the Internet at http://pubs.acs.org.

■ AUTHOR INFORMATION

Corresponding Authors

e.w.meijer@tue.nl
s-stupp@northwestern.edu

Notes

The authors declare no competing financial interest.

■ ACKNOWLEDGMENTS

This work was supported by the U.S. Department of Energy Basic Energy Sciences Program (grant DE-FG02-00ER45810), the European Research Council (FP7/2007-2013) ERC Grant Agreement and the Ministry of Education, Culture and Science (Gravity program 024.001.035). We thank the Advanced Photon Source (DOE Contract DE-AC02-06CH11357), Dr. Job Boekhoven for acquiring SEM images on freeze-dried PA samples, Dr. Tyson Moyer for SAXS data, and Dr. Patricia Y. W. Dankers and Dr. Tom F. A. de Greef for stimulating discussions.

■ REFERENCES

(1) (a) Aida, T.; Meijer, E. W.; Stupp, S. I. *Science* **2012**, *335*, 813. (b) Cui, H.; Webber, M. J.; Stupp, S. I. *Biopolymers* **2010**, *94*, 1.

(2) Silva, G. A.; Czeisler, C.; Niece, K. L.; Beniash, E.; Harrington, D. A.; Kessler, J. A.; Stupp, S. I. *Science* **2004**, *303*, 1352.

(3) Webber, M. J.; Tongers, J.; Renault, M.-A.; Roncalli, J. G.; Losordo, D. W.; Stupp, S. I. *Acta Biomaterialia* **2010**, *6*, 3.

(4) Tysseling-Mattiace, V. M.; Sahni, V.; Niece, K. L.; Birch, D.; 2008, *28*, 3814. Czeisler, C.; Fehlings, M. G.; Stupp, S. I.; Kessler, J. A. *J. Neurosci.* **2008**, *28*, 3814.

(5) Rajangam, K.; Behanna, H. A.; Hui, M. J.; Han, X.; Hulvat, J. F.; Lomasney, J. W.; Stupp, S. I. *Nano Lett.* **2006**, *6*, 2086.

(6) (a) Mata, A.; Geng, Y.; Henrikson, K. J.; Aparicio, C.; Stock, S. R.; Satcher, R. L.; Stupp, S. I. *Biomaterials* **2010**, *31*, 6004. (b) Spoerke, E. D.; Anthony, S. G.; Stupp, S. I. *Adv. Mater.* **2009**, *21*, 425. (c) Newcomb, C. J.; Bitton, R.; Velichko, Y. S.; Snead, M. L.; Stupp, S. I. *Small* **2012**, *8*, 2195. (d) Lee, S. S.; Huang, B. J.; Kaltz, S. R.; Sur, S.; Newcomb, C. J.; Stock, S. R.; Shah, R. N.; Stupp, S. I. *Biomaterials* **2013**, *34*, 452.

(7) Shah, R. N.; Shar, N. A.; Del Rosario Lim, M. M.; Hsieh, C.; Nuber, G.; Stupp, S. I. *Proc. Natl. Acad. Sci. U.S.A.* **2010**, *107*, 3293.

(8) (a) Lee, O.-S.; Cho, V.; Schatz, G. C. *Nano Lett.* **2012**, *12*, 4907. (b) Tovar, J. D.; Claussen, R. C.; Stupp, S. I. *J. Am. Chem. Soc.* **2005**, *127*, 7337. (c) Lee, O.-S.; Stupp, S. I.; Schatz, G. C. *J. Am. Chem. Soc.* **2011**, *133*, 3677. (d) Paramonov, S. E.; Jun, H.-W.; Hartgerink, J. D. *J. Am. Chem. Soc.* **2006**, *128*, 7291. (e) Pashuck, E. T.; Cui, H.; Stupp, S. I. *J. Am. Chem. Soc.* **2010**, *132*, 6041.

(9) Velichko, Y. S.; Stupp, S. I.; Olvera de la Cruz, M. *J. Phys. Chem. B* **2008**, *112*, 2326.

(10) (a) Hartgerink, J. D.; Beniash, E.; Stupp, S. I. *Science* **2001**, *294*, 1684. (b) Zhang, S.; Greenfield, M. A.; Mata, A.; Palmer, L. C.; Bitton, R.; Mantei, J. R.; Aparicio, C.; Olvera de la Cruz, M.; Stupp, S. I. *Nat. Mater.* **2010**, *9*, 594. (c) Pashuck, E. T.; Stupp, S. I. *J. Am. Chem. Soc.* **2010**, *132*, 8819.

(11) (a) Von Gröning, M.; De Feijter, I.; Stuart, M. C. A.; Voets, I. K.; Besenius, P. *J. Mater. Chem. B* **2013**, *1*, 2008. (b) Ghosh, A.; Haverick, M.; Stump, K.; Yang, X.; Tweedle, M. F.; Goldberger, J. E. *J. Am. Chem. Soc.* **2012**, *134*, 3647. (c) Boekhoven, J.; Koot, M.; Wezendonk, T. A.; Eelkema, R.; Van Esch, J. H. *J. Am. Chem. Soc.* **2012**, *134*, 12908.

(12) (a) Hayward, R. C.; Pochan, D. J. *Macromolecules* **2010**, *43*, 3577. (b) Moore, J. S.; Kraft, M. L. *Science* **2008**, *320*, 620. (c) Sorrells, J. L.; Tsai, Y.-H.; Wooley, K. L. *J. Polym. Sci., Part A: Polym. Chem.* **2010**, *48*, 4465. (d) Cui, H.; Chen, Z.; Zhong, S.; Wooley, K. L.; Pochan, D. J. *Science* **2007**, *317*, 647. (e) Huang, J.; Bonduelle, C.; Thévenot, J.; Lecommandoux, S.; Heise, A. *J. Am. Chem. Soc.* **2012**, *134*, 119. (f) Tidhar, Y.; Weissman, H.; Wolf, S. G.; Gulino, A.; Rybtchinski, B. *Chem.—Eur. J.* **2011**, *17*, 6068. (g) Hermans, T. M.; Broeren, M. A. C.; Gomopoulos, N.; Van Der Schoot, P.; Van Genderen, M. H. P.; Sommerdijk, N. A. J. M.; Fytas, G.; Meijer, E. W. *Nat. Nanotechnol.* **2009**, *4*, 721. (h) Kaeser, A.; Fischer, I.; Abbel, R.; Besenius, P.; Dasgupta, D.; Gillisen, M. A. J.; Portale, G.; Stevens, A. L.; Herz, L. M.; Schenning, A. P. H. J. *ACS Nano* **2013**, *7*, 408.

(13) McClendon, M. T.; Stupp, S. I. *Biomaterials* **2012**, *33*, 5713.

(14) Shimizu, S.; Shimizu, K. *J. Am. Chem. Soc.* **1999**, *121*, 2387.

(15) The red-shifted random coil spectra might include some α-helix characteristics as well. However, this spectrum is clearly not related to β-sheets, as is corroborated by DLS experiments.

(16) (a) Tanford, C. *Adv. Prot. Chem.* **1968**, *23*, 121. (b) Matthews, C. R. *Methods Enzymol.* **1987**, *154*, 498.

(17) Yanagi, K.; Ashizaki, M.; Yagi, H.; Sakurai, K.; Lee, Y.-H.; Goto, Y. *J. Biol. Chem.* **2011**, *286*, 23959.

(18) Korevaar, P. A.; Schaefer, C.; De Greef, T. F. A.; Meijer, E. W. *J. Am. Chem. Soc.* **2012**, *134*, 13482.

(19) It did not escape our attention that the driving forces for the assembly could change with solvent composition. In aqueous solutions, desolvation of the hydrophobic tails is anticipated to facilitate an entropy-driven assembly that increases with temperature. In higher HFIP contents, the assembly process becomes enthalpy-driven and weakens upon heating.